International Journal of Modern Physics C
Vol. 22, No. 10 (2011) 1093–1105

DOI: 10.1142/S0129183111016774

World Scientific
www.worldscientific.com

A SIMPLE ALGORITHM TO ENFORCE DIRICHLET BOUNDARY CONDITIONS IN COMPLEX GEOMETRIES

CHRISTIAN HUBER* and JOSEF DUFEK†

School of Earth and Atmospheric Sciences
Georgia Institute of Technology
311 Ferst Drive, Atlanta GA 30332, USA
**christian.huber@eas.gatech.edu*
†*josef.dufek@eas.gatech.edu*

BASTIEN CHOPARD

Computer Science Department, University of Geneva
CUI, 7 Route de Drize, 1227 Carouge, Switzerland
Bastien.Chopard@unige.ch

Received 10 December 2010
Accepted 22 August 2011

We present a new algorithm to implement Dirichlet boundary conditions for diffusive processes in arbitrarily complex geometries. In this approach, the boundary conditions around the diffusing object is replaced by the fictitious phase transition of a pure substance where the energy cost of the phase transition largely overwhelms the amount of energy stored in the system. The computing cost of this treatment of the boundary condition is independent of the topology of the boundary. Moreover, the implementation of this new approach is straightforward and follows naturally from enthalpy-based numerical methods. This algorithm is compatible with a wide variety of discretization methods, finite differences, finite volume, lattice Boltzmann methods and finite elements, to cite a few. We show, here, using both lattice Boltzmann and finite-volume methods that our model is in excellent agreement with analytical solutions for high symmetry geometries. We also illustrate the advantages of the algorithm to handle more complex geometries.

Keywords: Diffusion; Dirichlet boundary conditions; phase transition; complex geometry.

PACS Nos.: 11.25.Hf, 123.1K.

1. Introduction

Diffusion is an important process for chemical and heat transport. Both natural and engineering systems where diffusive processes occur can have a complex boundary topology. Enforcing boundary conditions (BC) (on flux or composition/temperature) on such complex boundaries requires an intensive numerical treatment where the diffusive flux out of the domain (tangential and normal to the boundary) has to be computed.[1,2] Ghost computational cells surrounding the

domain are generally introduced and the BC is enforced by using the desired constraint at the boundary (fixed concentration, fixed flux) and interpolating the scalar field values (for the diffusing field) around the ghost cells. In that respect, the equations solved for ghost cells are different from the nodes in the diffusing domain and can vary from a ghost cell to another depending on the topology of the boundary.

In this study, we focus on Dirichlet BCs (imposed composition/temperature) for the diffusion equation. We propose a model based on the enthalpy method, where we replace the BCs around the diffusing body with a fictitious phase transition. During the phase transition of pure substances, the temperature at the boundary is fixed and energy flux is partitioned into latent heat. This process provides the conceptual formulation for a general BC that fixes the value at an arbitrarily complex surface. By setting the latent heat associated with the phase transition to arbitrarily large values (compared to the "energy in the system"), the boundary between the two phases of the pure substance is fixed spatially and the phase transition will not be complete. This strategy allows us to replace the implementation of the Dirichlet BC with the simple calculation of a bulk property, the fictitious enthalpy, and the addition of a source/sink term defined in similar way at each node of the domain. In our model, the ghost cells surrounding the diffusing domain, where the diffusive flux is absorbed into a latent heat sink, behave identically to cells in the diffusing domain, and, therefore, do not require a special treatment.

In the next section, we describe in more detail the physical model (diffusion equation) and the enthalpy approach to the imposition of Dirichlet BCs. We then follow with a short description of two numerical methods we use to test our model, namely a LB and a finite-volume (FV) method. In the next section, we test the model against analytical solutions in simple geometries, such as diffusion out of an infinite slab or cylinder. We show an application which highlights the efficiency of our method to deal with a complex topology and which does not require any additional numerical treatment.

2. Mathematical Model

In this study, we focus on the two-dimensional (2D) or three-dimensional (3D) diffusion equation with a fixed temperature or concentration BC. Mass or energy conservation (we will use the latter one) in the absence of advection and phase change gives

$$\frac{\partial T}{\partial t} = \nabla \cdot (\kappa \cdot \nabla T), \tag{1}$$

where κ is the thermal diffusivity. Similarly, for the mass conservation of a chemical species C,

$$\frac{\partial C}{\partial t} = \nabla \cdot (D \cdot \nabla C), \tag{2}$$

where D is the molecular diffusivity of C.

The BC for the present case is

$$T(\mathbf{x}) = T_b \quad \text{or} \quad C(\mathbf{x}) = C_b \quad \mathbf{x} \in \delta V, \tag{3}$$

where δV is the arbitrarily complex boundary topology of the object. And we will assume the following initial condition

$$T(\mathbf{x}) = T_0 \quad \text{or} \quad C(\mathbf{x}) = C_0 \quad \mathbf{x} \in V \quad \text{at } t = 0. \tag{4}$$

We emphasize that the initial conditions are not required to be homogeneous and that $T_0 = T_0(\mathbf{x})$ without any loss of generality for the method presented here.

Using the equivalent formalism of Green's functions to solve for the 3D diffusion equation in a body of volume V with boundary S with initial concentration $T(x, 0)$ and fixed concentration T_b imposed on S,

$$T(\mathbf{x}, t) = \int_V \mathcal{G}(\mathbf{x}, t \mid \mathbf{x}', 0)\mathrm{dV}' - \underbrace{\kappa \int_0^t \mathrm{dt}' \int_S \mathrm{dS}'\, T_b(\mathbf{x}', t) \frac{\partial}{\partial n'} \mathcal{G}(\mathbf{x}, t \mid \mathbf{x}', t')}_{\text{boundary condition}}, \tag{5}$$

the role of the topology of the surface of the diffusing body on the solution (analytical or numerical) becomes more apparent. In Eq. (5), $\mathcal{G}$ is the Green's function for the diffusion equation that satisfies the BC (here fixed concentration) on S. The second integral of Eq. (5) highlights the complexity of solving a simple diffusion equation in bodies with arbitrary geometries, as the shape of the diffusing object influences the Green's function and its gradient normal to the surface S.

For simplicity, the following discussion focuses on heat diffusion, but the same approach applies to chemical diffusion as discussed below.

As illustrated in Fig. 1(a), let us consider a computational domain V, containing a substance S subject to an imposed temperature T_b on ∂V, the boundary of V. Let us immerse V in a bounding box $B = V \cup \bar{V}$, with periodic boundary condition, as shown in Fig. 1(b). The problem of solving the heat equation on V with Dirichlet BC on ∂V can be transformed into a problem of solving the heat equation on B with the same pure substance S, but assuming that S can be in two possible phases, say solid on $\bar{V}$ and liquid on V.

To describe these two phases, we introduce a new variable $0 \leq \phi(x, t) \leq 1$, the melt fraction. When $\phi = 1$ the substance is entirely liquid, and when $\phi = 0$, it is entirely solid.

Initially we will assume that in $\bar{V}$, the substance is in the solid state, $\phi = 0$, at a melting temperature T_m which is chosen as $T_m = T_b$. In V, we assume that S is at a higher temperature $T_0 > T_b$, in a liquid phase with $\phi = 1$.

We know from thermodynamics that, due to the latent heat, the temperature of S is fixed to T_b at any point x where there is a mix of liquid and solid phases, i.e. where $0 < \phi < 1$. Therefore, if the points $x \in \partial V$ are in such a state during all the heat transfer process, the interface between V and $\bar{V}$ will act as a Dirichlet BC. If the Stefan number $\mathcal{S} = c(T_m - T_0)/L$ is chosen small enough, the time needed to

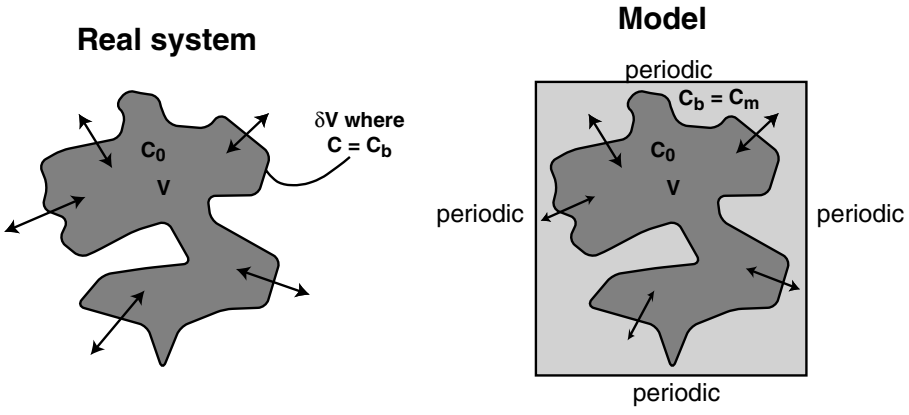

Fig. 1. Illustration of the enthalpy-based method to implement Dirichlet BCs on arbitrary geometries. The computation of the BCs on the surface of the diffusing object δV is replaced by the calculation of a phase transition of a pure substance. In this method, the object V and its surroundings are modeled as two different phases of the same pure substance and the latent heat is set such that the phase transition does not progress and remains fixed spatially. (a) Real system. (b) Model.

fully solidify gridpoints in V or fully melt the gridpoints in $\bar{V}$ can be made arbitrarily lengthened and the simulated Dirichlet conditions will hold for the entire computation.

A thermal, two-phase system can be described by the enthalpy $H = cT + L\phi$, where c is the specific heat and L the latent heat. The heat equation is then modified to

$$\frac{\partial H}{\partial t} = \nabla(\kappa c \nabla T) \quad \text{or} \quad \frac{\partial T}{\partial t} + \frac{L}{c}\frac{\partial \phi}{\partial t} = \nabla(\kappa \nabla T), \tag{6}$$

indicating that the heat flux $J_Q = -\kappa \nabla T$ is responsible for the variation of H.

The method we propose to implement a Dirichlet BC using a two-phase substance results from the decomposition in two steps of the change of enthalpy over a time Δt. First we assume that the temperature changes due to both the heat flux and the variation of the melt fraction ϕ. Second, the resulting departure of T from the fixed temperature T_b causes a variation of the melt fraction to readjust to the correct heat distribution.

The first step is a simple time discretization of Eq. (6), where the melt fraction appears as a source term

$$T(\mathbf{x}, t + \Delta t) = T(\mathbf{x}, t) + \Delta t \nabla(\kappa \nabla T) - \frac{L}{c}(\phi(\mathbf{x}, t) - \phi(\mathbf{x}, t - \Delta t)). \tag{7}$$

The second step implements the fact that the heat $c(T - T_b)$ that has been incorrectly stored as specific heat is now transformed into latent heat by changing the

melt fraction by an amount $L\Delta\phi = L(\phi(t+1) - \phi(t))$

$$\phi(\mathbf{x}, t+\Delta t) = \begin{cases} 0 & \text{if } \phi(\mathbf{x},t) + \dfrac{c}{L}(T(\mathbf{x}, t+\Delta t) - T_b) < 0, \\ 1 & \text{if } \phi(\mathbf{x},t) + \dfrac{c}{L}(T(\mathbf{x}, t+\Delta t) - T_b) > 1, \\ \phi(\mathbf{x},t) + \dfrac{c}{L}(T(\mathbf{x}, t+\Delta t) - T_b) & \text{otherwise.} \end{cases} \tag{8}$$

This variation of ϕ will then readjust the temperature at the next iteration, thanks to the source term in Eq. (7).

Note that the above method can be applied identically to chemical diffusion; then the fictitious enthalpy function becomes

$$H(x,t) = cC(x,t) + L\phi(x,t), \tag{9}$$

where c is a physically meaningless equivalent of the specific heat for concentration that allows us to set up a modified Stefan number $\mathcal{S} = c(C_0 - C_m)/L \ll 1$. In this case, the equivalent of the melting temperature C_m is the fixed concentration at the boundary δV, i.e. $C_b = C_m$.

The enthalpy approach discussed here can be applied to any type of diffusion equation solver, as proposed in the next section.

3. Numerical Models

3.1. *Lattice Boltzmann model*

In this section, we explain how the two-phase method presented in the previous section can be implemented in a LB framework. For an in-depth description of LB methods, the reader is referred to Refs. 3–7. The implementation we propose here is similar to the enthalpy method presented in Refs. 8 and 9, where LB schemes are used to describe the propagation of a melting front. Other methods of phase change using a phase-field equation have been successfully applied to solidification and crystal growth.[10]

Following the enthalpy method, an additional scalar field ϕ is introduced on each lattice node, from which the local enthalpy is defined as $H(\mathbf{x},t) = cT(\mathbf{x},t) + L\phi(x,t-1)$. Following Eq. (7), the standard LB model for diffusion[3,11,12] can be modified to include a source term

$$f_i(\mathbf{x}+\mathbf{e}_i, t+1) = f_i(\mathbf{x},t) - \frac{1}{\tau_h}(f_i(\mathbf{x},t) - f_i^{\text{eq}}(\mathbf{x},t)) - w_i\frac{L}{c}(\phi(\mathbf{x},t) - \phi(\mathbf{x},t-1)), \tag{10}$$

where the melt fraction ϕ evolves according to Eq. (8).

In Eq. (10), the temperature is calculated from the sum of the particle distribution functions $T(\mathbf{x},t) = \sum_i f_i(\mathbf{x},t)$. The quantities w_i are the lattice weights, c_s^2 the lattice sound speed and τ_h is the relaxation time that relates to the diffusivity

as $\kappa = c_s^2(\tau_h - 1/2)$. The unit vectors $\mathbf{e}_i$ correspond to the lattice directions and $f_i^{\mathrm{eq}} = w_i T$ are the so-called local equilibrium distributions.

In the Appendix, it is shown that this LB enthalpy method reduces to a very simple numerical scheme where, on $\bar{V}$, the post-collision local equilibrium distributions are redefined according to T_b, without however modifying the post-collision non-equilibrium distribution. As a result, $\phi(\mathbf{x})$ can be considered as a static flag indicating whether a point $\mathbf{x}$ is in V or in $\bar{V}$.

3.2. *Finite-volume model*

We implement a standard FV approach to discretize the time-dependent diffusion equation with source term (latent heat or fictitious concentration source).[13] To solve for the diffusion equation in the two-dimensional domain we implement an iterative solution procedure [alternating directions implicit (ADI)]. A predictor-corrector method was used to compute the partitioning of the energy into sensible and latent heat during the phase change process.[14] The procedure used here was modified from the approach of Dufek and Bergantz.[15]

4. Results

In this section, we use analytical solutions (approximations to the infinite series solutions) for the diffusive loss from an infinite plane sheet (slab) and infinite cylinder. The outside of the cylinder or sheet is assumed to be a perfect absorbent of heat/mass and remains at a fixed temperature, composition throughout the diffusion process. In all calculations, the Stefan number (the efficiency of the method to absorb the flux out of the diffusing body) was set to 10^{-8}. We chose to compare the results obtained with both numerical method to the fractional loss from these simple geometries as it provides a good test to validate the time, and implicitly, the spatial dependence of our modeling results.

The fraction of heat/mass lost by diffusion for an initially homogeneous infinite plane sheet with fixed boundary temperature/concentration (here assumed to be 0 for simplicity) is given by[16]

$$f \simeq \begin{cases} \dfrac{2}{\sqrt{\pi}} \left(\dfrac{Dt}{r^2}\right)^{1/2} & 0 \le f \le 0.6, \\ 1 - \dfrac{8}{\pi^2} \exp\left(-\dfrac{\pi^2 Dt}{4r^2}\right) & 0.45 \le f \le 1, \end{cases} \tag{11}$$

where r is the half-width of the plane sheet (infinite slab). Similarly, the fraction loss by diffusion for an initially homogeneous infinite cylinder of radius r is given by[16]

$$f \simeq \begin{cases} \dfrac{4}{\sqrt{\pi}} \left(\dfrac{Dt}{r^2}\right)^{1/2} - \dfrac{Dt}{r^2} & 0 \le f \le 0.6, \\ 1 - \dfrac{9}{13} \exp\left(-\dfrac{5.78 Dt}{r^2}\right) & 0.6 \le f \le 1. \end{cases} \tag{12}$$

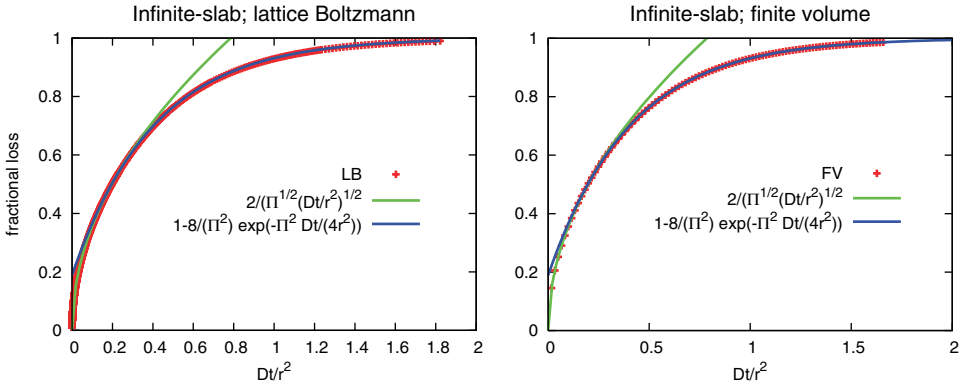

Fig. 2. Comparison between the analytical solution and the numerical model for the diffusive flux out of an infinite slab of thickness r. The diffusive loss is shown in terms of the initial fraction of heat or chemical component remaining in the slab. Time is made dimensionless using the Fourier number $\mathcal{F} = Dt/r^2$. The left panel shows the results we obtain with the LB model and the right panel with the FV model.

Starting with LB method, we first compare the analytical solution for the fractional loss by an infinite slab [Eq. (11)] with the results obtained from our boundary condition model. Figure 2 shows the time evolution of the fraction of heat/concentration lost by the sheet with the two asymptotes of Eq. (11). The agreement is excellent for both numerical methods, even if the resolution here is fairly small, the half-width of the slab is discretized over 25 nodes only.

Our boundary condition model is also tested against analytical solutions for an infinite cylinder of radius r. The results for the LB calculations are shown in the left panel of Fig. 3 together with the analytical solutions of Eq. (12). For comparison, the results obtained with the FV approach are shown in the right panel.

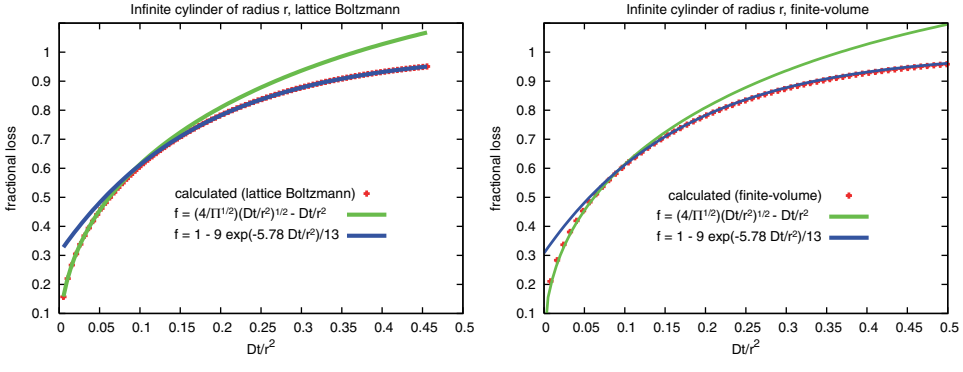

Fig. 3. Comparison between the analytical solution and the LB (left panel) and FV (right panel) numerical models for the diffusive flux out of an infinite cylinder of radius r. The diffusive loss is shown in terms of the initial fraction of heat or chemical component remaining in the slab. Time is made dimensionless using the Fourier number $\mathcal{F} = Dt/r^2$.

It is noteworthy to mention that the spatial discretization of the curvature of the cylinder is done with steps, i.e. on a uniform grid G with no interpolation between nodes for the position of the boundary. More precisely, $\mathbf{x} \in G$ is a part of the cylinder if and only if $|\mathbf{x} - \mathbf{c}|^2 < r^2$, where $\mathbf{c} \in G$ is the center of the cylinder.

Although the radius is only $r = 25$ nodes, the results obtained with both numerical methods — the LB and the FV method — are in excellent agreement with the theory. We show below that the accuracy is actually second order in the grid spacing. This might be surprising as the discretization procedure to resolve the cylinder shape is manifestly first order. However, if one considers that the effective location of the boundary is off-lattice and precisely on the circle of radius r, then the accuracy is second order.

To test the order of accuracy of the method (for the LB algorithm) we compare the diffusive loss outside of the infinite cylinder against a more accurate approximation of the analytical solution[17]

$$F \simeq \frac{4}{\sqrt{\pi}}\left(\frac{Dt}{r^2}\right)^{1/2} - \frac{Dt}{r^2} - \frac{1}{3\sqrt{\pi}}\left(\frac{Dt}{r^2}\right)^{3/2} - 0.244122\left(\frac{Dt}{r^2}\right)^{2} \quad 0 \leq f \leq 0.78, \tag{13}$$

for different resolution R. The resolution R is simply defined here to be the ratio of the size of the radius of the cylinder in number of lattice nodes (>25) to the radius in a reference run (25 nodes). The error in the prediction of the cumulative diffusive flux out of the cylinder is defined as

$$\delta_F = \frac{1}{N}\sum_{i=1}^{N}\frac{|F_{\mathrm{an},i} - F_{\mathrm{calc},i}|}{F_{\mathrm{an},i}}, \tag{14}$$

where N is the number of timesteps required to reach $F = 0.78$ (we found that most of the error accumulates before 60−80% loss). $F_{\mathrm{an},i}$ and $F_{\mathrm{calc},i}$ are respectively the cumulative fractional losses at timestep i for the analytical solution [Eq. (13)] and the numerical calculations with the LB model. Figure 4 shows that the relationship between the accuracy of the method and the resolution used is second order. The arbitrary position of the boundary of the cylinder with respect to the square lattice, i.e. every node outside of a radius of 25, 50, 75, and 100 nodes was set to be outside the diffusing body, is usually typical of first-order method. This suggests that the method is more accurate than expected, at least for the case of a cylinder. Future work will be required to characterize the order of this new boundary condition approach.

5. Discussion

The advantages of our algorithm to implement Dirichlet type BCs stems from its simplicity and ease of implementation. It is based on the replacement of the intense node-specific treatment required to enforce these BCs, especially on complex geometries, with a generic model of phase transition that applies identically to every node of the computational domain, boundary or not. Our model, however, requires

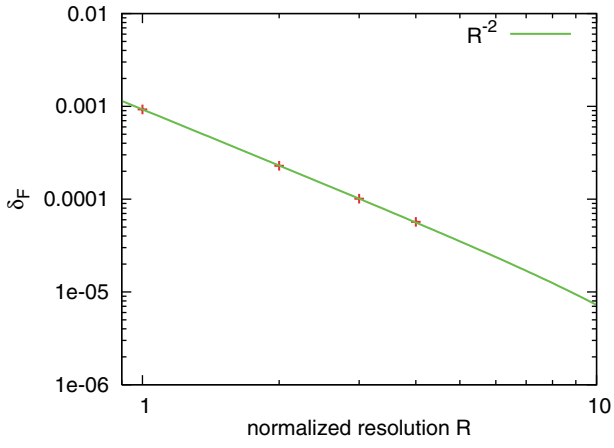

Fig. 4. Error on the cumulative diffusive flux out of an infinite cylinder of radius r between the analytical solution of Eq. (13) and the lattice Boltzmann model for different resolution factors R. The error $\delta_F \sim R^{-2}$.

the presence of additional nodes around the object that are treated as the other phase of the pure substance. As such they act as a perfectly efficient sponge, or, as an infinite reservoir for diffusive fluxes directed respectively out or into the object. Two additional scalar fields are required (the fictitious enthalpy and solid fraction) at each node of the computational domain. However, we show a way to circumvent this problem for the LB model in the Appendix. We show that the boundary condition can be enforced with a modified collision and does not require these additional scalar fields. In that case, the only additional computational cost of the model is to expand the size of the computational domain by a few nodes outside of the diffusing domain (ghost cells). The additional computing cost, in 2D, is about $k * P/(nx\, ny)$, where k is the width of the latent heat buffer zone around the object in number of grid nodes (about two nodes for example), P is the perimeter of the object and nx, ny the number of nodes in the diffusing domain. The periodic BCs on cells at the edges of the enlarged domain can be treated easily. Time-dependent boundary values [e.g. $T_b = T_b(t)$] are allowed in the model, the only limitation is that T_b has to remain homogeneous (no spatial variation along the boundary) to avoid diffusion between boundary nodes.

For all the computations made for this study, the enthalpy and melt fraction calculation required a single iteration per timestep to converge within the level of accuracy displayed in Figs. 2 and 3. Huber *et al.*[18] showed that multiple iterations are required only when the Stefan number is greater than 1, as in our case $\mathcal{S} \ll 1$, a single iteration is expected to yield an accurate treatment of the boundary condition. We found that the choice of $\mathcal{S}$ does not affect the stability or accuracy of the method (as long as $\mathcal{S} \ll 1$). The maximum $\mathcal{S}$ that one can use, and, that allows to enforce the fixed boundary condition, varies with the domain size and initial conditions. A rule of thumb is to make sure that the initial "sensible heat" integrated

over the volume of the diffusing body, i.e. the initial enthalpy of the domain, is smaller than the latent heat that can be absorbed by the nodes bounding the object

$$\int_V cT(t=0)dV < \int_{\bar{V}} Ld\bar{V}. \tag{15}$$

The implementation of Dirichlet BCs with an enthalpy-based method for a fictitious phase transition allows us to treat every computational node identically, i.e. the calculations are the same everywhere in the computational domain. This becomes advantageous when dealing with diffusing bodies with complex topologies, because the method does not require any specific treatment for the complicated boundary.

A wide range of engineering or geological applications require solving the diffusion equation in domains bounded by an idealized fixed (sometimes controlled) temperature/concentration condition. The topology of these bodies can be complex, for example heat or molecular diffusion in natural minerals or heat transfer in components of electric circuits. In the next section, we show an application of the model to the diffusion of radiogenic chemical elements out of a prismatic mineral with pyramidal termination. We emphasize that the code used here is identical (except adapted for 3D) to the one used above for the much simpler and more symmetrical geometries.

6. Application

In natural systems, the topology of the physical domain over which diffusion occurs can be arbitrarily complex. In geosciences, solid-state diffusion in mineral phases can yield very important information about the absolute age (geochronometry using radioactive elements) and/or the time−temperature pathway of the sample (cooling evolution of a sample above the closure temperature). In engineering, the efficiency of the cooling of electronic components in circuits, requires an efficient method to handle heat conduction with fixed temperatures boundaries. In this section, we discuss briefly an application of our method taken from geosciences.

Some naturally occurring minerals contain a measurable mass fraction of radioactive isotopes such as ^{40}K and ^{238}U. As the decay constants of these radioactive elements have been measured accurately, it is possible to use the parent−daughter ratio (here ^{40}K/^{40}Ar or ^{238}U/^{234}Th) as a clock to measure the age of the sample. The laboratory procedure that allows to measure the mass ratio between the parent and daughter elements consists of subjecting the sample (mineral) to different degassing steps at different temperatures (between a few hundreds to a thousand degrees in general) for a few minutes/hours in a vacuum chamber.[19] The high temperature allows for faster diffusion of each element in the sample (molecular diffusivity generally depends exponentially on temperature), and the mass of each elements leaving the mineral at each step is measured by a mass-spectrometer. In order to relate the mass released during each heating step to a

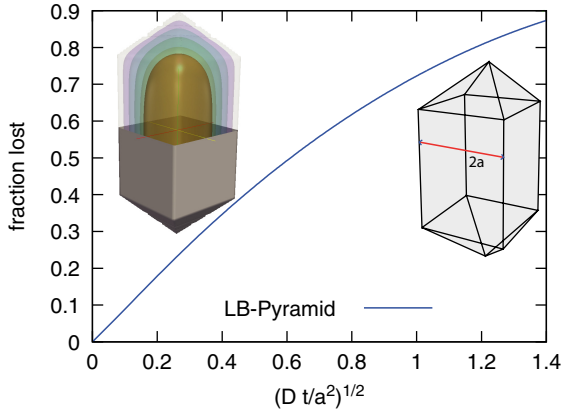

Fig. 5. Application of diffusion with fixed concentration/temperature for a mineral with a prismatic basis and pyramidal terminations. This conceptual example is relevant to the degassing of natural minerals (for example zircons) where the absolute age of the mineral can be measured from the diffusion of helium out of the sample during laboratory procedures. Time is made dimensionless with the Fourier number as Dt/a^2, where D is the elemental diffusivity of helium (in this particular case), a is a reference length-scale in the mineral. Modified from Huber *et al.*[18]

diffusivity and potentially an age, one needs to use a diffusion model with fixed concentration ($= 0$, vacuum) at the vacuum−mineral boundary. The boundary condition model we propose here allows for a simple treatment of the boundary when solving for the diffusion equation and estimate the mass released for each element during each laboratory step. In Fig. 5, we show an application of our model where the diffusion equation, with Dirichlet BCs, is solved in a mineral with a square basis and pyramidal terminations (like a zircon mineral). The figure shows the mass fraction of daughter product loss with dimensionless time. The two insets illustrate the temporal evolution of a contour surface with a fixed concentration of radiogenic element (left inset) and a schematic illustration of the reference length-scale a used to define the dimensionless time Fo.

7. Conclusion

We present a novel method to implement Dirichlet BCs for the diffusion equation. The enforcement of the fixed concentration/temperature along complex boundaries is replaced by a conceptual model where the boundary becomes the interface between the object and a reservoir that represent the two phases of a pure substance during a phase transition. By imposing that the latent heat overwhelms the available energy for the phase transition in our fictitious model, we fix the interface spatially between the two phases, and ensure that it remains at the temperature/concentration consistent with the stability of the two coexisting phases. This method allows us to apply an identical procedure for each node of the extended computational domain irrespective to its nature as a part of the diffusing body or its

boundary. Avoiding the usage of a special treatment for the boundary of diffusing body proves to be very efficient when solving the diffusion equation in arbitrarily complex geometries. This method is moreover applicable to any discretization scheme and partial differentiation equation solver.

Acknowledgments

C. Huber was funded by Swiss postdoctoral fellowship PBSKP2-128477 and J. Dufek was funded by NSF 0838200.

Appendix

In this Appendix, we show that the enthalpy-based method applied to the LB Bhatnagar−Gross−Krook (BGK) model can be implemented in a simple way by combining Eqs. (8) and (10).

At the boundary between the object of volume V and its latent heat "reservoir" $\bar{V}$, where $0 \leq \phi(\mathbf{x}, t-1) + c(T(\mathbf{x}, t) - T_b)/L \leq 1$, we have

$$f_i(\mathbf{x} + \mathbf{e}_i, t+1) = f_i(\mathbf{x}, t) + \frac{1}{\tau_H}(f_i^{\mathrm{eq}}(\mathbf{x}, t) - f_i(\mathbf{x}, t)) - \omega_i(T(\mathbf{x}, t) - T_b), \tag{A.1}$$

everywhere else, the evolution equation is

$$f_i(\mathbf{x} + \mathbf{e}_i, t+1) = f_i(\mathbf{x}, t) + \frac{1}{\tau_H}(f_i^{\mathrm{eq}}(\mathbf{x}, t) - f_i(\mathbf{x}, t)). \tag{A.2}$$

Using the definition of the equilibrium distribution f_i^{eq} and expanding the distribution into equilibrium and non-equilibrium parts, we get

$$f_i = f_i^{\mathrm{eq}} + f_i^{\mathrm{neq}} = \omega_i T + f_i^{\mathrm{neq}}. \tag{A.3}$$

Using the shorthand notation $f_i^{\mathrm{out}} \equiv f_i(\mathbf{x} + \mathbf{e}_i, t+1)$ and $f_i^{\mathrm{in}} \equiv f_i(\mathbf{x}, t)$, we see that Eq. (16) becomes

$$\begin{aligned} f_i^{\mathrm{out}} &= \omega_i T_b + \left(1 - \frac{1}{\tau_H}\right) f_i^{\mathrm{neq}} \\ &= f_i^{\mathrm{eq}}(T_b) + \left(1 - \frac{1}{\tau_H}\right) f_i^{\mathrm{neq}}. \end{aligned} \tag{A.4}$$

This shows that the enthalpy method builds a post-collision distribution with the equilibrium part fixed at the boundary temperature and scales the non-equilibrium part (which is related to diffusive fluxes) with a factor $(1 - 1/\tau_H)$. In contrast, the evolution of a non-boundary site can be expanded to

$$f_i^{\mathrm{out}} = f_i^{\mathrm{eq}}(T^{\mathrm{in}}) + \left(1 - \frac{1}{\tau_H}\right) f_i^{\mathrm{neq}}, \tag{A.5}$$

where $T^{\mathrm{in}} = T(\mathbf{x}, t)$. The enthalpy method proposed here can be replaced by an equivalent and simpler approach that does not require to introduce new fields such

as melt fraction or enthalpy where the collision is replaced by Eq. (19) on the sites marked by a boundary flag. It also shows that in our model imposing a Dirichlet BC on arbitrarily complex geometries imposes the right temperature/concentration at the boundary and also does not affect the diffusive fluxes at the boundary (no effect on the non-equilibrium part of the distribution).

References

1. R. Mittal and G. Iaccarino, *Annu. Rev. Fluid Mech.* **37**, 239 (2005).
2. C. S. Peskin, *Annu. Rev. Fluid Mech.* **14**, 345 (1981).
3. B. Chopard and M. Droz, *Cellular Automata Modeling of Physical Systems* (Cambridge Univ. Press, 1998).
4. D. A. Wolf-Gladrow, *Lattice-Gas Cellular Automata and Lattice Boltzmann Models: An Introduction*, Lect. Notes Math. (Springer, 2000), p. 308.
5. S. Succi, *The Lattice Boltzmann Equation, For Fluid Dynamics and Beyond* (Oxford Univ. Press, New york, 2001).
6. R. Benzi, S. Succi and M. Vergassola, *Phys. Rep.* **222**, 145 (1992).
7. S. Chen and G. Doolen, *Annu. Rev. Fluid Mech.* **30**, 329 (1998).
8. W.-S. Jiaung, J.-R. Ho and C.-P. Kuo, *Numer. Heat Transf.: Part B* **39**, 167 (2001).
9. C. Huber, A. Parmigiani, B. Chopard, M. Manga and O. Bachmann, *Int. J. Heat Fluid Flow* **29**, 1469 (2008).
10. I. Rasin, W. Miller and S. Succi, *Phys. Rev. E* **72**, 066705 (2005).
11. B. Chopard, P. Luthi and A. Dupuis, *Adv. Complex Syst.* **5**, 103 (2002).
12. P. Bhatnagar, E. Gross and A. Krook, *Phys. Rev.* **94**, 511 (1954).
13. S. V. Patankar, *Numerical Heat Transfer and Fluid Flow* (Taylor and Francis, 1980), p. 197.
14. V. R. Voller and C. R. Swaminathan, *Numer. Heat Transf. B* **19**, 175 (1991).
15. J. Dufek and G. W. Bergantz, *J. Petrol.* **46**, 2167 (2005).
16. J. Crank, *The Mathematics of Diffusion*, 2nd edn (Oxford Univ. Press, USA, 1980), p. 424.
17. E. B. Watson, K. H. Wanser and K. A. Farley, *Geochim. Cosmochim. Acta* **74**, 614 (2010).
18. C. Huber, W. S. Cassata and P. R. Renne, *Geochim. Cosmochim. Acta* (2011), doi: 10.1016/j.gca.2011.01.039.
19. C. Allègre, *Isotope Geology* (Cambridge Univ. Press, 2008).